Interaction between Anillin and RacGAP50C connects the actomyosin contractile ring with spindle microtubules at the cell division site

Pier Paolo D'Avino[1,*], Tetsuya Takeda[1], Luisa Capalbo[1], Wei Zhang[2], Kathryn S. Lilley[2], Ernest D. Laue[2] and David M. Glover[1]

[1]Cancer Research UK Cell Cycle Genetics Research Group, Department of Genetics, University of Cambridge, Downing Street, Cambridge, CB2 3EH, UK
[2]Department of Biochemistry, University of Cambridge, 80 Tennis Court Road, Cambridge, CB2 1GA, UK
*Author for correspondence (e-mail: p.davino@gen.cam.ac.uk)

Accepted 24 January 2008
Journal of Cell Science 121, 1151-1158 Published by The Company of Biologists 2008
doi:10.1242/jcs.026716

Summary

Anillin, one of the first factors recruited to the cleavage site during cytokinesis, interacts with actin, myosin II and septins, and is essential for proper organization of the actomyosin contractile ring. We employed affinity-purification methodology coupled with mass spectrometry to identify Anillin-interacting molecules in *Drosophila* cells. We isolated several actin and myosin proteins, three of the five *Drosophila* septins and RacGAP50C (Tum), a component of the centralspindlin complex. Using drug and RNA interference (RNAi) treatments we established that F-actin is essential for Anillin cortical localization in prometaphase but not for its accumulation at the cleavage furrow after anaphase onset. Moreover, septins were not recruited to the cleavage site in cells in which *Anillin* was knocked down by RNAi, but localized to central-spindle microtubules, suggesting that septins travel along microtubules to interact with Anillin at the furrow. Finally, we demonstrate that RacGAP50C is necessary for Anillin accumulation at the furrow and that the two proteins colocalize in vivo and interact in vitro. Thus, in addition to its role in activating RhoA signalling, RacGAP50C also controls the proper assembly of the actomyosin ring by interacting with Anillin at the cleavage furrow.

Supplementary material available online at
http://jcs.biologists.org/cgi/content/full/121/8/1151/DC1

Key words: Anillin, Centralspindlin, Affinity purification, Protein complex

Introduction

In many organisms, the assembly and contraction of actomyosin filaments drives the formation and ingression of the cleavage furrow during cytokinesis. Several lines of evidence indicate that the Rho family of small GTPases controls this cytoskeletal rearrangement (D'Avino et al., 2005; Piekny et al., 2005). In particular, RhoA activation by a RhoGEF known as Pebble (Pbl) in *Drosophila* and ECT2 in mammals is thought to be the major signalling event responsible for furrow initiation (Bement et al., 2005; Kimura et al., 2000; Nishimura and Yonemura, 2006; Prokopenko et al., 1999; Tatsumoto et al., 1999; Yuce et al., 2005). Compelling evidence in both flies and mammals indicates that this activation requires the interaction of the RhoGEF Pbl/ECT2 with the RacGAP component of the centralspindlin complex, known as RacGAP50C (or Tum) in *Drosophila* and MgcRacGAP in mammals (Kamijo et al., 2006; Nishimura and Yonemura, 2006; Somers and Saint, 2003; Yuce et al., 2005; Zhao and Fang, 2005). This evolutionary conserved two-protein complex localizes to the plus ends of microtubules and is essential for the assembly of an array of antiparallel and interdigitating microtubules – the central spindle, which forms between separating anaphase chromosomes (Mishima et al., 2002). The other component, dubbed Pavarotti (Pav-KLP) in *Drosophila* and MKLP-1 in mammals, is a kinesin-like protein that displays plus-end-directed motor activity (Adams et al., 1998; Nislow et al., 1992; Powers et al., 1998; Raich et al., 1998). Successful furrowing, however, requires the actomyosin filaments to be assembled properly in order to drive the ingression of the equatorial cortex and its associated plasma membrane (Eggert et al., 2006). Several lines of evidence indicate that the cytoskeletal protein Anillin (also known as Scraps in flies) plays a key role in the assembly of the actomyosin contractile ring and its interaction with the furrowing membrane. First, this protein has been shown to bind actin, myosin II and septins (Field and Alberts, 1995; Kinoshita et al., 2002; Straight et al., 2004). Furthermore, the presence of a pleckstrin homology (PH) domain at its C-terminus suggests that it might interact with the plasma membrane (Field and Alberts, 1995). Finally, *Drosophila* and mammalian cells depleted of Anillin display disorganized contractile rings and failure of late cytokinesis (Somma et al., 2002; Straight et al., 2004). In order to gain novel insights into Anillin functions and regulation during cytokinesis, we used affinity purification coupled with mass spectrometry to identify factors that interact with this protein in *Drosophila* cells. We isolated several interactors, including all the *Drosophila* actin proteins, several myosin proteins, three of the five fly septins and RacGAP50C. By using a combination of RNAi, drug treatments, in vitro binding and in vivo localization assays, we demonstrate that the RacGAP component of the centralspindlin complex interacts directly with Anillin after anaphase onset and that Anillin in turn recruits at least two septins, Peanut (Pnut) and Septin 2 (Sep2). Our findings indicate that

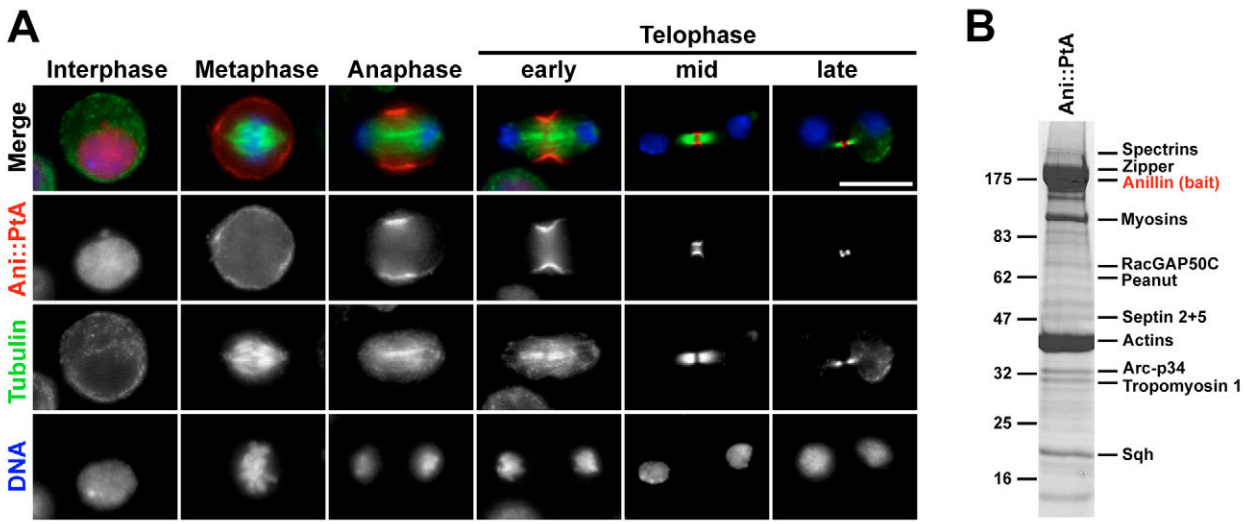

Fig. 1. Isolation of proteins interacting with Anillin in *Drosophila* cells. (A) Cells stably expressing the *Ani::PtA* transgene were fixed and stained to detect Protein A (red in merged panels), tubulin (green in merged panels) and DNA (blue in merged panels). (B) Colloidal Coomassie-stained gel of one the two purifications from *Ani::PtA* cells. The position of some of the proteins identified by mass spectrometry (MS) is indicated on the right (also see Table 1). The bait, Ani::PtA, is in red. The numbers on the left indicate the size in kD of the molecular-weight marker. Scale bar: 10 μm.

RacGAP50C not only promotes actomyosin filament assembly via RhoA activation, but also their proper organization into a contractile ring during cytokinesis.

Results and Discussion

Identification of Anillin interactors by affinity purification

To purify Anillin along with its in vivo associated partners, we established a *Drosophila* stable cell line expressing this protein tagged at its C-terminus with two IgG-binding domains of the Protein A (PtA). Ani::PtA was distributed in a manner that was indistinguishable from the endogenous protein: it localized to the nucleus in interphase, to the cortex in prometaphase and metaphase, and it then accumulated at the equatorial region in anaphase and at the cleavage furrow during telophase (Fig. 1A) (Field and Alberts, 1995). Unfortunately, no protocols are currently available for synchronizing *Drosophila* tissue-culture cells at different mitotic stages. However, we have shown that treatment with the proteasome inhibitor MG132 induces an increase in the mitotic index (D'Avino et al., 2007; Przewloka et al., 2007). We therefore treated Ani::PtA cells with MG132, and then affinity-purified the tagged protein and interacting partners as previously described (Fig. 1B) (Chen et al., 2007; D'Avino et al., 2007; Przewloka et al., 2007). After purification, the proteins were identified by mass spectrometry. A partial list showing the major proteins identified in two distinct purifications is given in Table 1. As expected, we identified all the *Drosophila* actin proteins, and the heavy and light chains of the non-muscle myosin II, dubbed Zipper and Spaghetti squash (Sqh), respectively (Fig. 1B, Table 1). Interestingly, although not surprisingly, two other myosin proteins, 31DF and 61F, were also identified among the strongest interactors, along with Tropomyosin 1 and Arc-p34, the 34-kD component of the Arp2/3 complex. We also identified three of the five septins encoded by the *Drosophila* genome (Fig. 1B, Table 1). Sep2 and Pnut showed the highest scores and were therefore analyzed further (see below). Unexpectedly, we also identified the three *Drosophila* spectrin proteins as very strong hits in our purifications. None of these proteins, however, were found to accumulate at the cleavage furrow during cytokinesis, and their depletion by RNAi, either separately or in all possible combinations, did not affect Anillin localization during mitosis and cytokinesis (supplementary material Fig. S1 and data not shown). Thus, it seems likely that the spectrins were pulled-down because of their strong affinity for actin. One very intriguing result was the identification of RacGAP50C, one of the two components of the centralspindlin complex (Fig. 1B, Table 1) (Somers and Saint, 2003). Its motor partner, Pav-KLP, was also identified in our Ani::PtA purifications, albeit with a much lower score (Table 1), suggesting that Anillin might interact more strongly with RacGAP50C than with Pav-KLP. The identification of RacGAP50C was very significant considering

Table 1. List of the major proteins identified by mass spectrometry that interact with Anillin in *Drosophila* cells

Protein	Score	Peptides
Actin 5C	1483	784
Actin 42A	1470	778
Actin 57B	1010	468
Actin 79B	812	401
Actin 87E	981	466
Actin 88F	941	439
Anillin (Scraps)	3166	175
Arc-p34	934	41
Myosin HC (Zipper)	7303	767
Myosin LC (Sqh)	855	283
Myosin 31DF	3215	119
Myosin 61F	3076	172
Pav-KLP	37	2
RacGAP50C	1132	30
Septin 2	226	5
Septin 3 (Peanut)	184	5
Septin 5	43	3
α-Spectrin	6597	167
β-Spectrin	4536	121
βH-Spectrin (Karst)	2459	57
Tropomyosin I	519	10

The proteins shown in Fig. 1B are listed along with their relative MS score and number of peptides. The bait, Ani::PtA, is in red.

that we isolated this protein in only two other purifications out of more than fifty different pull-down assays using PtA-tagged mitotic baits that localized to diverse subcellular locations including the mitotic and central spindle, the cleavage furrow, kinetochores and centrosomes (data not shown) (Chen et al., 2007; D'Avino et al., 2007; Przewloka et al., 2007). One of the other baits that identified RacGAP50C was its PtA-tagged motor partner Pav-KLP (data not shown).

RacGAP50C and Anillin colocalize at the plus ends of microtubules during cytokinesis

Centralspindlin accumulates at the plus ends of microtubules after anaphase onset thanks to the motor activity of Pav-KLP, whereas Anillin localizes to the cell cortex soon after nuclear envelope break-down (Fig. 1A) (D'Avino et al., 2006; Field and Alberts, 1995; Somers and Saint, 2003). Thus, our mass-spectrometry results (Fig. 1B, Table 1) raised the intriguing hypothesis that Anillin could interact with the RacGAP50C pool present at the microtubule plus ends of a sub-population of spindle microtubule that contact the equatorial cortex after anaphase onset, the 'peripheral' microtubules (Inoue et al., 2004). In this way, RacGAP50C could also be responsible for the recruitment and/or maintenance of Anillin at the cleavage furrow. Consistent with this hypothesis, previous studies have shown that Anillin does not accumulate at the equatorial cortex after knockdown of *RacGAP50C* by RNAi (*RacGAP50C* RNAi) or in *RacGAP50C* mutants (Somma et al., 2002; Zavortink et al., 2005), whereas RacGAP50C localization to the spindle midzone was unaffected in Anillin-depleted cells (supplementary material Fig. S2). We reasoned that the initial localization of Anillin to the cortex in prometaphase might depend on its strong affinity for F-actin. Indeed, the two colocalize throughout mitosis and cytokinesis, although F-actin remained also at the cortical polar regions during telophase (supplementary material Fig. S3) (Field and Alberts, 1995). To test this hypothesis, we treated cells for 1 hour with 20 μM Latranculin-A (Lat-A), a concentration sufficient to completely depolymerize F-actin (Dean et al., 2005). Because, under our conditions, completion of furrow ingression takes about 20-30 minutes after anaphase onset (D'Avino et al., 2006), this treatment ensured that every fixed cell observed in anaphase or early-to-mid-telophase had been deprived of F-actin, from before the onset of chromosome segregation. We noticed that, after Lat-A treatment, interphase cells underwent a remarkable cell-shape change and displayed very long microtubule bundles in interphase (supplementary material Fig. S4). A similar cell-shape change was also observed in a different *Drosophila* cell line after RNAi depletion of actin genes or treatment with another actin-depolymerizing drug (Eggert et al., 2004). This suggests that the mesh of cortical F-actin can inhibit microtubule polymerization, similar to recent findings in *Drosophila* oocytes (Dahlgaard et al., 2007). Consistent with our initial hypothesis, Anillin failed to localize cortically in Lat-A-treated metaphase cells, but was still able to accumulate at the equatorial region after anaphase onset (Fig. 2A,B). However, Anillin no longer formed a continuous band at the equatorial cortex, but instead showed a patchy and/or filamentous distribution. Some of these Anillin patches organized in rod-like structures that appeared to localize to microtubule plus-ends (Fig. 2A,B). Because the centralspindlin complex is also known to localize to the plus ends of microtubules (D'Avino et al., 2006; Somers and Saint, 2003), we co-stained Lat-A-treated cells for Anillin and RacGAP50C. We consistently observed that the two proteins colocalized at the cortex after anaphase onset in control DMSO-treated cells and at the rod-like structures observed after Lat-A treatment, although Anillin also displayed a patchy membrane localization that was clearly independent of RacGAP50C (Fig. 2B). We also incubated cells for 48 hours with dsRNA directed against *RacGAP50C* (D'Avino et al., 2006), and then treated them with Lat-A for 1 hour. As previously described (Somma et al., 2002), Anillin did not accumulate at the equatorial cortex after RacGAP50C depletion but was either dispersed along the whole cortex or simply excluded from the polar regions in DMSO-treated cells (Fig. 2C). More importantly, the vast majority of *RacGAP50C* RNAi telophase cells (85.3%; n=163) did not exhibit the Anillin rod-like structures at the microtubule plus ends after Lat-A treatment, even though Anillin still displayed a patchy and/or filamentous accumulation at the cortex (Fig. 2C). Altogether, these data suggest that Anillin localized to the microtubule plus ends after Lat-A treatment through its interaction with RacGAP50C.

Note that failure of Anillin recruitment to the equatorial region after *RacGAP50C* RNAi cannot simply result from the lack of furrow ingression typical of these cells because Lat-A-treated cells also failed to initiate furrowing but nevertheless showed restricted localization of Anillin at the equatorial cortex (Fig. 2A,B).

Although Anillin consistently failed to accumulate at the equator in RacGAP50C-depleted cells, it was often still excluded from one or both cortical polar regions (Fig. 2C). A previous report indicated that this 'polar exclusion' did not occur after RhoA depletion (Somma et al., 2002). This would indicate that, as already proposed for myosin, the polar exclusion of Anillin might be caused, directly or indirectly, by the cell elongation that accompanies spindle elongation during anaphase B (Dean et al., 2005; Hickson et al., 2006). This cell-shape change seems to require the RhoA-ROK pathway, but not RacGAP50C (Dean et al., 2005; Hickson et al., 2006).

Anillin interacts with RacGAP50C in vitro

To test whether Anillin could directly bind RacGAP50C, we investigated whether the two proteins interact in vitro. We were unable to produce a recombinant full-length Anillin protein in *Escherichia coli*, most likely because of its considerable size, and therefore decided to express four separate GST-tagged fragments, A1 to A4, that covered the entire length of the protein (Fig. 3A). These fragments were then used in a pull-down assay with a [^{35}S]-methionine-labelled RacGAP50C polypeptide generated by in vitro transcription and translation. We reasoned that the GAP domain was unlikely to be necessary for interaction with Anillin, and so truncated this polypeptide immediately downstream of the C1 (phorbol ester/diacylglycerol binding) motif, at residue 371 (Fig. 3C). We found that a C-terminal Anillin fragment, A4, could specifically pull down the labelled RacGAP50C$_{1\text{-}371}$ peptide (Fig. 3A). A3 also interacted, but this was much weaker than A4 (Fig. 3A). This result indicated that Anillin was able to directly bind RacGAP50C in vitro via its C-terminal region. To confirm these findings and further narrow down the binding sites, we also expressed three different Anillin truncations tagged with GFP in *Drosophila* tissue-culture cells (Fig. 3B). A truncated protein lacking only the PH domain, Ani$_{1\text{-}1104}$, had a distribution identical to full-length Anillin (Fig. 3B and supplementary material Fig. S5A; compare with Fig. 1A). It localized to the nucleus in interphase, to the cortex in metaphase and to the cleavage furrow after anaphase onset (Fig. 3B and supplementary material Fig.

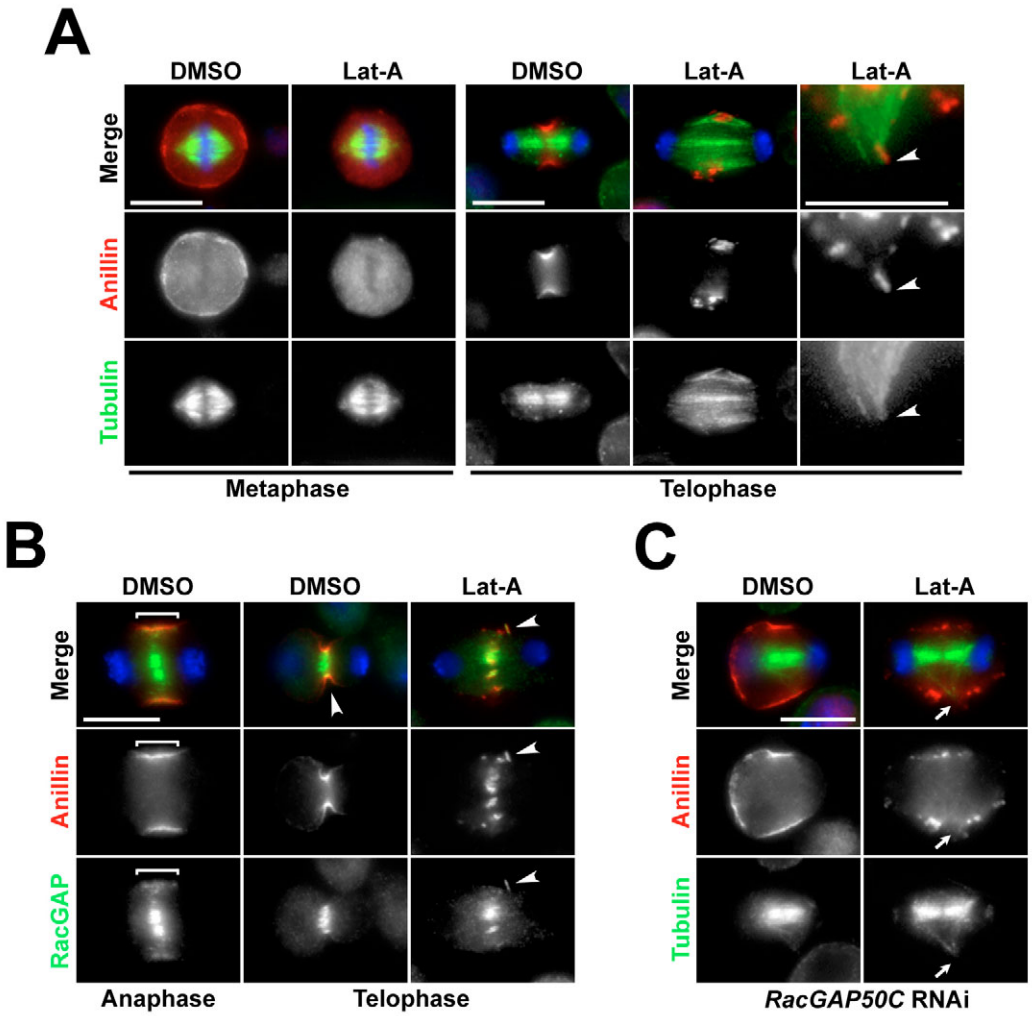

Fig. 2. Colocalization of Anillin and RacGAP50C during cell division. (A) Cells were treated with DMSO (control) or Lat-A for 1 hour, and were then fixed and stained to detect Anillin (red in merged panels), tubulin (green in merged panels) and DNA (blue in merged panels). The rightmost panels show a magnification of the microtubules contacting the equatorial cortex in a Lat-A-treated cell; the spindle axis and chromosomes are not contained in this field. The arrowhead marks Anillin localization at the microtubule plus ends. (B) Cells were treated with DMSO (control) or Lat-A for 1 hour, and were then fixed and stained to detect Anillin (red in merged panels), RacGAP50C (green in merged panels) and DNA (blue in merged panels). The bracket and arrowheads mark the sites of Anillin and RacGAP50C colocalization (orange/yellow in merged panels). Note the colocalization at the microtubule plus ends in Lat-A-treated cells. (C) Cells were first incubated with dsRNA directed against *RacGAP50C* for 48 hours and then treated with DMSO (control) or Lat -A for 1 hour. The samples were then fixed and stained to detect Anillin (red in merged panels), tubulin (green in merged panels) and DNA (blue in merged panels). Note the absence of Anillin rod-shaped structure at the microtubule plus ends (marked by the arrow) in Lat-A-treated cells. Scale bars: 10 μm.

S5A). A fragment comprising the sequence between the actin-binding domain and the PH motif, $Ani_{410\text{-}1104}$, still localized to the nucleus in interphase, but it no longer accumulated at the cortex after nuclear envelope break-down (supplementary material Fig. S5B), supporting the above finding that F-actin is necessary for Anillin cortical localization (Fig. 2). Strikingly, this fragment was also found at the spindle midzone (i.e. the overlapping plus ends of the central spindle) (Fig. 3B, arrowheads), in which it colocalized with RacGAP50C (supplementary material Fig. S6). This result is consistent with $Ani_{410\text{-}1104}$ being able to bind RacGAP50C. The fragment comprising residues 410-766 displayed nuclear localization during interphase but did not localize to either the cortex or the spindle midzone (Fig. 3B and supplementary material Fig. S5C). Thus, the combination of both in vitro binding and in vivo localization experiments indicated that the region important for binding to RacGAP50C must reside between residues 766 and 1104, and most likely between residues 929 and 1104, just upstream of the Anillin PH domain (Fig. 3A,B). Interestingly, this section of the protein contains a region that displays the highest homology among different species (Fig. 3A) (Oegema et al., 2000).

To identify the RacGAP domain(s) necessary for binding Anillin, we tested different peptides translated and labelled in vitro with [^{35}S] methionine. As shown in Fig. 3C, the $RacGAP50C_{1\text{-}135}$ fragment containing the coiled-coil domain and the regions known to bind Pav-KLP and Pbl (Somers and Saint, 2003), did not show any specific binding, whereas $RacGAP50C_{136\text{-}371}$ was specifically pulled down by the Anillin A4 fragment. The $RacGAP50C_{136\text{-}242}$ fragment also failed to bind A4, whereas $RacGAP50C_{205\text{-}371}$ showed a weaker interaction compared with $RacGAP50C_{136\text{-}371}$

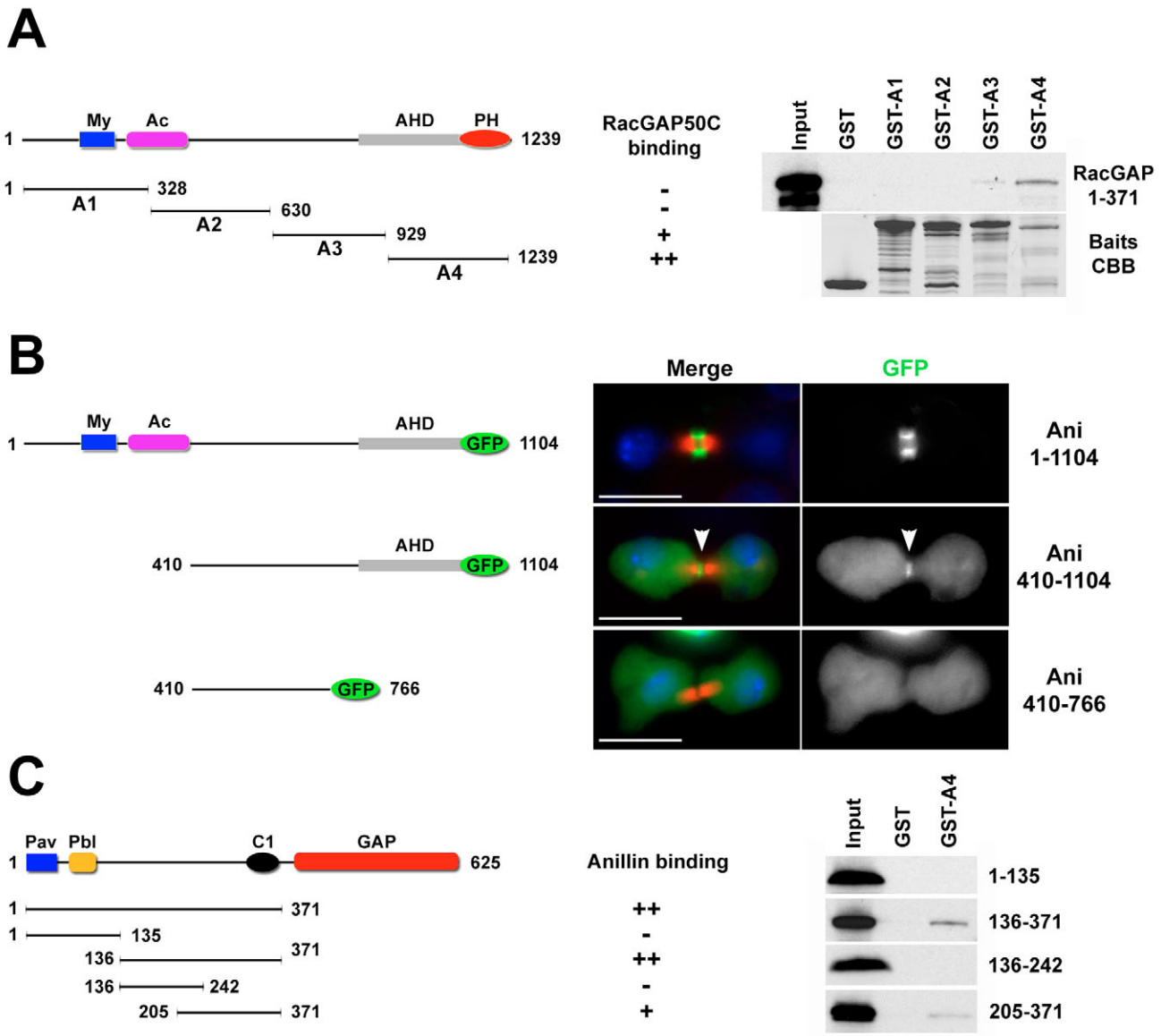

Fig. 3. Anillin and RacGAP50C interact in vitro. (A) At the left is shown a schematic representation of the full-length Anillin protein and of the several fragments used for in vitro binding assays. The PH domain and myosin (My)- and actin (Ac)-binding regions are indicated. The thick grey line marks the region showing the highest homology among different species (Anillin Homology Domain, AHD). The autoradiograph of the pull-down assay along with a Coomassie-stained gel (CBB) showing the amounts of bait proteins used for the binding assay are shown at the right. The top bands in the Coomassie gel correspond to the full-length GST-tagged baits. (B) Subcellular localization of GFP-tagged Anillin fragments. A schematic description of the fragment tagged with GFP is shown at the left and their relative subcellular localization at the right. The cells were fixed and stained to detect tubulin (red in merged panels), GFP (green in merged panels) and DNA (blue in merged panels). The arrowhead marks the spindle midzone localization of $Ani_{410\text{-}1104}$. (C) At the left is shown a schematic representation of the full-length RacGAP50C protein and of the several fragments used for in vitro binding assays. The GAP and C1 domains, and Pav-KLP (Pav)- and Pebble (Pbl)-binding regions are indicated. The autoradiographs of the pull-down assays are shown at the right. The amount of GST and GST-A4 proteins used is the same as in A. Scale bar: 10 μm.

(Fig. 3C). Taken together, these results demonstrate that the region upstream of the Anillin PH domain is able to interact in vitro with a motif in RacGAP50C that is distinct from the region containing the binding sites for Pav and Pbl.

In conclusion, we surmise that Anillin initially localizes to the cortex after mitotic entry because of its strong affinity for F-actin (Fig. 2A, Fig. 3B and supplementary material Fig. S5). Then, after anaphase onset, at least two distinct mechanisms co-operate to localize Anillin at the furrow. The first, mediated by Rho but independent of RacGAP50C, excludes Anillin from the polar regions, probably as a result of cell elongation, as already shown for myosin (Dean et al., 2005; Hickson et al., 2006). The second involves a direct interaction with RacGAP50C, which restricts and maintains the localization of Anillin to the cleavage site during furrow ingression (Fig. 2B,C and Fig. 3).

Anillin is required for septin recruitment to the cleavage furrow

As mentioned above, three of the five *Drosophila* septins – Pnut, Sep2 and Septin 5 (Sep5) – were identified in our pull-down assays (Fig. 1B, Table 1). A fourth septin, Septin 1 (Sep1), was detected

only in one of the two separate purifications and with a very low score, making its identification more uncertain. Although the interaction between Anillin and septins has already been described in another system (Kinoshita et al., 2002), it was previously unclear which of the five *Drosophila* septins could complex with Anillin. Interestingly, the two showing the highest scores, Pnut and Sep2, are also the only two septins that were identified in a genome-wide screen for genes required for cytokinesis in *Drosophila* cultured cells (Echard et al., 2004). We analyzed the localization of Pnut and Sep2 after *Anillin* RNAi (Fig. 4A). We could not analyze Sep5 localization because no antibodies are currently available. Moreover, its high homology with Sep2 (~70%), and the low score and number of peptides obtained from mass-spectrometry analysis, made its identification as an interacting protein dubious. Western blot analysis indicated that Anillin could not be detected after a 48-hour incubation with dsRNA (Fig. 4B). Both Pnut and Sep2 failed to localize to the cleavage site in these *Anillin*-depleted cells, and instead localized to the central-spindle microtubules in a significant percentage (30-40%) of telophase cells (Fig. 4A). Because these two septins, unlike Anillin, did not accumulate to the cortex after nuclear envelope break-down (supplementary material Fig. S7), our results suggest that Pnut and Sep2 travel along the central-spindle microtubules to be delivered to the cortex, in which they then interact with Anillin. A similar failure to recruit Pnut to the cleavage furrow was also observed in *scraps* (*Anillin*) mutant embryos, although mislocalization to the central spindle was not reported by these authors (Field et al., 2005). Conversely, Anillin localization during cytokinesis was unaffected in cells incubated for 96 hours with dsRNAs directed against either *pnut* or *Sep2*, or against both septins simultaneously (Fig. 4C). Western blot analysis confirmed that the expression of both septins was severely reduced after our RNAi treatment (Fig. 4D). Interestingly, the expression of Pnut was reduced after *Sep2* RNAi and vice-versa, suggesting that depletion of one septin can affect the stability of the other, consistent with the observation that these two septins are found in a three-protein complex along with Sep1 (Field et al., 1996). Our results indicated that severe depletion of Pnut and Sep2 did not compromise Anillin localization during cytokinesis. No significant increase in the number of multinucleate cells, however, was detected in our septin-depleted cells and telophase figures appeared normal (Fig. 4C). This is in accord with two previous reports showing that septin RNAi treatments for either 3 or 4 days did not cause cytokinesis failure (Eggert et al., 2004; Somma et al., 2002). However, Echard at al. (Echard at al., 2004) reported an

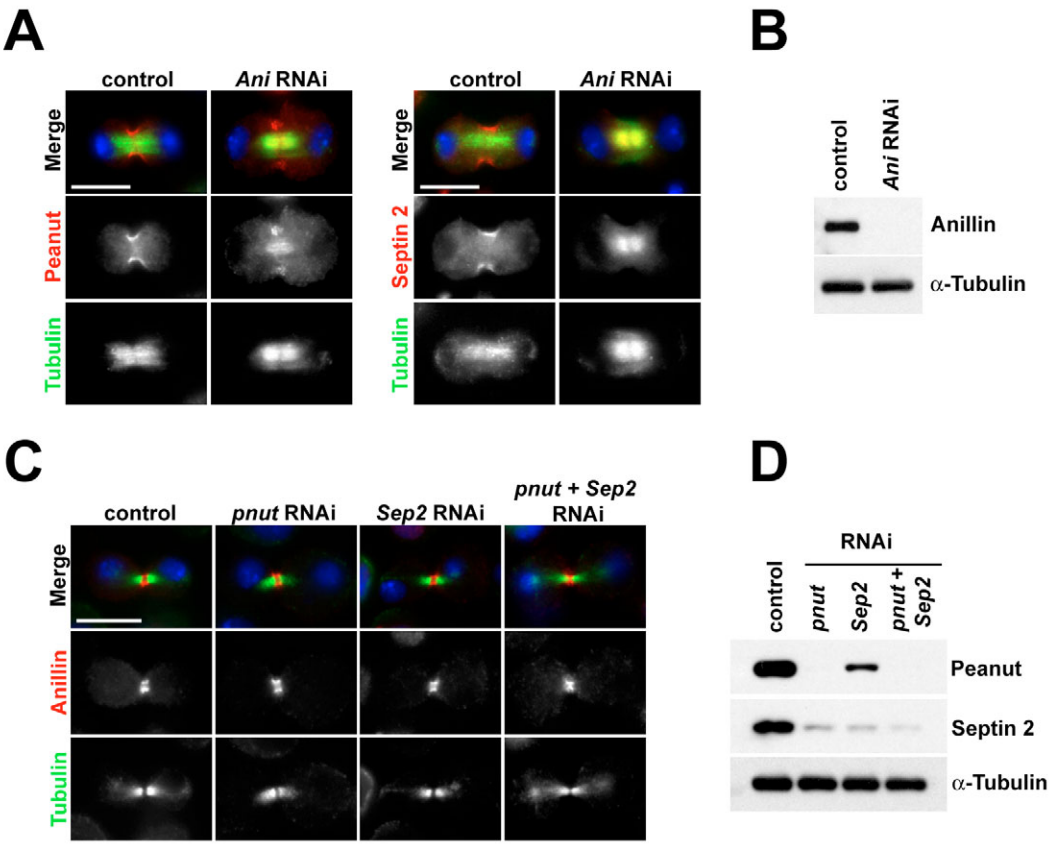

Fig. 4. Anillin recruits Pnut and Sep2 to the cleavage furrow. (A) Cells were treated for 48 hours with dsRNAs directed against either *Anillin* or GFP (control), and were then fixed and stained to detect tubulin (green in merged panels), DNA (blue in merged panels) and either Pnut or Sep2 (red in merged panels). (B) Western blot analysis of protein levels after RNAi treatment. Cells were incubated with dsRNAs directed against either *Anillin* or GFP (control). After 48 hours the proteins were extracted and separated on a 10% SDS gel, transferred onto a PVDF membrane and probed with antibodies against Anillin and α-tubulin. (C) Cells were treated for 96 hours with dsRNAs directed against GFP (control), *pnut*, *Sep2* or both septins simultaneously, and then fixed and stained to detect Anillin (red in merged panels), tubulin (green in merged panels) and DNA (blue in merged panels). (D) Western blot analysis of protein levels after RNAi treatment. Cells were incubated with dsRNAs directed against GFP (control), *pnut*, *Sep2* or both septins simultaneously. After 96 hours the proteins were extracted and separated on a 10% SDS gel, transferred onto a PVDF membrane and probed with antibodies against Pnut, Sep2 and α-tubulin. Scale bar: 10 μm.

increase in cytokinesis defects when cells were exposed to dsRNAs against *pnut* or *Sep2* for a longer period (6 days). The difference in incubation time might very well explain the discrepancy between these two conflicting sets of results.

A connection between the actomyosin ring and the peripheral central-spindle microtubules during cytokinesis

In summary, we conclude that, after anaphase onset, Anillin directly binds RacGAP50C to establish a connection between the actomyosin filaments responsible for furrow ingression and a sub-population of spindle microtubule that contact the equatorial cortex, the peripheral microtubules (Figs 2 and 3) (Inoue et al., 2004). This interaction appears necessary to restrict and/or maintain the localization of Anillin to the cleavage site during furrowing (Fig. 2). In turn, Anillin recruits at least two septins, Pnut and Sep2 (Fig. 4). These proteins then form a scaffold necessary for proper organization of the actomyosin filaments and their interaction with the plasma membrane (Eggert et al., 2006). These data also provide a molecular mechanism for our previous observation that a membrane-tethered version of RacGAP50C could generate ectopic furrows that contained both Anillin and Pnut (D'Avino et al., 2006). Thus, RacGAP50C not only activates RhoA during cytokinesis through its interaction with the RhoGEF Pbl, but also binds Anillin at the furrow to control the proper organization of the actomyosin contractile ring. These results further support a model in which the RacGAP component of the centralspindlin complex acts as a key regulator of furrow formation and ingression, and so represents a major furrow-inducing signal (D'Avino et al., 2005; Saint and Somers, 2003).

Materials and Methods

Cell culture, RNAi and drug treatments, DNA constructs and generation of stable cell lines

The DMEL strain of S2 cells (Invitrogen) was used in all the experiments. These cells have been adapted to grow in serum-free medium (SFM). Generation of dsRNAs and RNAi treatments were performed as described previously (D'Avino et al., 2006; D'Avino et al., 2004). We specifically amplified DNA regions that, according to the information available from FlyBase (http://flybase.bio.indiana.edu/), were not expected to trigger off-target effects. Oligonucleotide sequences are available upon request.

For Lat-A treatment, cells were plated on coverslips for 2 hours and then treated for 1 hour with either Lat-A (Invitrogen) at a final concentration of 20 μM or with an equal volume of its solvent DMSO (Sigma) as a control.

Plasmids expressing Ani::PtA and the various GFP-tagged Anillin or RacGAP50C fragments under the control of the Actin5C or metallothionein promoters were constructed used Gateway technology (Invitrogen) as described previously (Chen et al., 2007; D'Avino et al., 2007; D'Avino et al., 2006). Stable cell lines were generated using blasticidin selection as previously published (D'Avino et al., 2006).

Microscopy

Immunocytochemistry was carried out as previously described (D'Avino et al., 2006; D'Avino et al., 2004). The Anillin, α-tubulin, Pnut and rabbit anti-RacGAP50C antibodies and their respective working dilution were as described previously (D'Avino et al., 2006; D'Avino et al., 2004). The rat anti-RacGAP50C antibody was a kind gift from R. Saint (University of Adelaide, Australia) and was used at 1:200 dilution. The rabbit anti-Sep2 antibody was a kind gift from J. Pringle (Stanford University, CA), and was used at a dilution of 1:40 and 1:400 for immunofluorescence and western blot, respectively. The mouse anti-α-spectrin antibody was obtained from the Developmental Studies Hybridoma Bank and the rabbit anti-β- and -β_H-spectrin antibodies were a gift from R. Dubreuil (University of Illinois at Chicago, IL) and were used as described (Dubreuil et al., 1997). Ani::PtA was detected using Texas Red ChromPure rabbit IgG (Jackson ImmunoResearch).

Protein-affinity purifications and mass spectrometry

Protein-A affinity purification was performed as previously described with minor modifications (Chen et al., 2007; D'Avino et al., 2007; Przewloka et al., 2007). The proteasome inhibitor MG132 (Sigma) was added to the SFM medium at a final concentration of 20 μM and cells incubated for 6 hours before collection. On average, 10^9 cells were used in each purification. The proteins were separated on either a 4-20% or 8-16% acrylamide gel, and the bands excised and analyzed by liquid-chromatography–mass-spectrometry (LC-MS)/MS as described previously (Chen et al., 2007; D'Avino et al., 2007; Przewloka et al., 2007). The MS/MS fragmentation data achieved was used to search the National Center for Biotechnology Information and FlyBase databases using the MASCOT search engine (http://www.matrixscience.com). Probability-based MASCOT scores were used to evaluate identifications. Only matches with $P<0.05$ for random occurrence were considered significant.

In vitro binding assay

Anillin fragments were generated by PCR and cloned into pGEX4T-TEV, a pGEX4T plasmid modified with the addition of a TEV cleavage site (a kind gift from M. Mishima, The Gurdon Institute, Cambridge, UK), to express N-terminal GST tagged polypeptides in *E. coli*. The GST-tagged products were then purified using glutathione sepharose 4B according to the manufacturer's instruction (GE Healthcare). [^{35}S]-methionine-labelled RacGAP50C fragments were prepared from corresponding PCR fragments amplified with primers harbouring a T7 promoter, and were then transcribed and translated in vitro using the TnT T7 Quick Coupled Transcription/Translation Systems (Promega) in the presence of [^{35}S]-methionine. Generally, 25 μl of glutathione sepharose beads containing purified GST-Anillin fragments were mixed with 5 μl of [^{35}S]-methionine-labelled RacGAP50C fragments and 300 μl of NET-N+ buffer (50 mM Tris-HCl, pH 7.4, 150 mM NaCl, 5 mM EDTA, 0.5% NP-40, and a cocktail of proteinase inhibitors commercially available from Roche) and incubated in ice for 30 minutes with periodic agitation. The mixture was then washed five times by adding 500 μl of NET-N+ buffer followed by centrifugation at 1500 rpm in a tabletop centrifuge for 1 minute. Beads were resuspended in 25 μl of 2× SDS sample buffer and typically one fifth of the mixture (10 μl) was loaded on 4-20% tris-glycine gel (Invitrogen). Proteins were then transferred onto a nitrocellulose membrane using the iBlot dry blotting system (Invitrogen) and exposed to X-ray films at –80°C.

We are grateful to R. Dubreuil, C. Field, M. Mishima, J. Pringle and R. Saint for antibodies and reagents. We thank M. Savoian for critical reading of the manuscript. This work was supported by a CR-UK programme grant to D.M.G., and a BBSRC project grant to D.M.G., E.D.L., K.S.L. and P.P.D.

Note added in proof

While this manuscript was under review, two related papers were published, one reporting the interaction between Anillin and RacGAP50C (Gregory et al., 2008) and the other studying Anillin behaviour after F-actin disassembly (Hickson and O'Farrell, 2008).

References

Adams, R. R., Tavares, A. A., Salzberg, A., Bellen, H. J. and Glover, D. M. (1998). *pavarotti* encodes a kinesin-like protein required to organize the central spindle and contractile ring for cytokinesis. *Genes Dev.* **12**, 1483-1494.

Bement, W. M., Benink, H. A. and von Dassow, G. (2005). A microtubule-dependent zone of active RhoA during cleavage plane specification. *J. Cell Biol.* **170**, 91-101.

Chen, F., Archambault, V., Kar, A., Lio, P., D'Avino, P. P., Sinka, R., Lilley, K., Laue, E. D., Deak, P., Capalbo, L. et al. (2007). Multiple protein phosphatases are required for mitosis in Drosophila. *Curr. Biol.* **17**, 293-303.

Dahlgaard, K., Raposo, A. A., Niccoli, T. and St Johnston, D. (2007). Capu and Spire assemble a cytoplasmic actin mesh that maintains microtubule organization in the Drosophila Oocyte. *Dev. Cell* **13**, 539-553.

D'Avino, P. P., Savoian, M. S. and Glover, D. M. (2004). Mutations in sticky lead to defective organization of the contractile ring during cytokinesis and are enhanced by Rho and suppressed by Rac. *J. Cell Biol.* **166**, 61-71.

D'Avino, P. P., Savoian, M. S. and Glover, D. M. (2005). Cleavage furrow formation and ingression during animal cytokinesis: a microtubule legacy. *J. Cell Sci.* **118**, 1549-1558.

D'Avino, P. P., Savoian, M. S., Capalbo, L. and Glover, D. M. (2006). RacGAP50C is sufficient to signal cleavage furrow formation during cytokinesis. *J. Cell Sci.* **119**, 4402-4408.

D'Avino, P. P., Archambault, V., Przewloka, M. R., Zhang, W., Lilley, K. S., Laue, E. and Glover, D. M. (2007). Recruitment of Polo kinase to the spindle midzone during cytokinesis requires the Feo/Klp3A complex. *PLoS ONE* **2**, e572.

Dean, S. O., Rogers, S. L., Stuurman, N., Vale, R. D. and Spudich, J. A. (2005). Distinct pathways control recruitment and maintenance of myosin II at the cleavage furrow during cytokinesis. *Proc. Natl. Acad. Sci. USA* **102**, 13473-13478.

Dubreuil, R. R., Maddux, P. B., Grushko, T. A. and MacVicar, G. R. (1997). Segregation of two spectrin isoforms: polarized membrane-binding sites direct polarized membrane skeleton assembly. *Mol. Biol. Cell* **8**, 1933-1942.

Echard, A., Hickson, G. R., Foley, E. and O'Farrell, P. H. (2004). Terminal cytokinesis events uncovered after an RNAi screen. *Curr. Biol.* **14**, 1685-1693.

Eggert, U. S., Kiger, A. A., Richter, C., Perlman, Z. E., Perrimon, N., Mitchison, T. J. and Field, C. M. (2004). Parallel chemical genetic and genome-wide RNAi screens identify cytokinesis inhibitors and targets. *PLoS Biol.* **2**, e379.

Eggert, U. S., Mitchison, T. J. and Field, C. M. (2006). Animal cytokinesis: from parts list to mechanisms. *Annu. Rev. Biochem.* **75**, 543-566.
Field, C. M. and Alberts, B. M. (1995). Anillin, a contractile ring protein that cycles from the nucleus to the cell cortex. *J. Cell Biol.* **131**, 165-178.
Field, C. M., al-Awar, O., Rosenblatt, J., Wong, M. L., Alberts, B. and Mitchison, T. J. (1996). A purified Drosophila septin complex forms filaments and exhibits GTPase activity. *J. Cell Biol.* **133**, 605-616.
Field, C. M., Coughlin, M., Doberstein, S., Marty, T. and Sullivan, W. (2005). Characterization of anillin mutants reveals essential roles in septin localization and plasma membrane integrity. *Development* **132**, 2849-2860.
Gregory, S. L., Ebrahimi, S., Milverton, J., Jones, W. M., Bejsovec, A. and Saint, R. (2008). Cell division requires a direct link between microtubule-bound RacGAP and Anillin in the contractile ring. *Curr. Biol.* **18**, 25-29.
Hickson, G. R. and O'Farrell, P. H. (2008). Rho-dependent control of Anillin behavior during cytokinesis. *J. Cell Biol.* **180**, 285-294.
Hickson, G. R., Echard, A. and O'Farrell, P. H. (2006). Rho-kinase controls cell shape changes during cytokinesis. *Curr. Biol.* **16**, 359-370.
Inoue, Y. H., Savoian, M. S., Suzuki, T., Mathe, E., Yamamoto, M. T. and Glover, D. M. (2004). Mutations in orbit/mast reveal that the central spindle is comprised of two microtubule populations, those that initiate cleavage and those that propagate furrow ingression. *J. Cell Biol.* **166**, 49-60.
Kamijo, K., Ohara, N., Abe, M., Uchimura, T., Hosoya, H., Lee, J. S. and Miki, T. (2006). Dissecting the role of Rho-mediated signaling in contractile ring formation. *Mol. Biol. Cell* **17**, 43-55.
Kimura, K., Tsuji, T., Takada, Y., Miki, T. and Narumiya, S. (2000). Accumulation of GTP-bound RhoA during cytokinesis and a critical role of ECT2 in this accumulation. *J. Biol. Chem.* **275**, 17233-17236.
Kinoshita, M., Field, C. M., Coughlin, M. L., Straight, A. F. and Mitchison, T. J. (2002). Self- and actin-templated assembly of Mammalian septins. *Dev. Cell* **3**, 791-802.
Mishima, M., Kaitna, S. and Glotzer, M. (2002). Central spindle assembly and cytokinesis require a kinesin-like protein/RhoGAP complex with microtubule bundling activity. *Dev. Cell* **2**, 41-54.
Nishimura, Y. and Yonemura, S. (2006). Centralspindlin regulates ECT2 and RhoA accumulation at the equatorial cortex during cytokinesis. *J. Cell Sci.* **119**, 104-114.
Nislow, C., Lombillo, V. A., Kuriyama, R. and McIntosh, J. R. (1992). A plus-end-directed motor enzyme that moves antiparallel microtubules in vitro localizes to the interzone of mitotic spindles. *Nature* **359**, 543-547.
Oegema, K., Savoian, M. S., Mitchison, T. J. and Field, C. M. (2000). Functional analysis of a human homologue of the Drosophila actin binding protein anillin suggests a role in cytokinesis. *J. Cell Biol.* **150**, 539-552.
Piekny, A., Werner, M. and Glotzer, M. (2005). Cytokinesis: welcome to the Rho zone. *Trends Cell Biol.* **15**, 651-658.
Powers, J., Bossinger, O., Rose, D., Strome, S. and Saxton, W. (1998). A nematode kinesin required for cleavage furrow advancement. *Curr. Biol.* **8**, 1133-1136.
Prokopenko, S. N., Brumby, A., O'Keefe, L., Prior, L., He, Y., Saint, R. and Bellen, H. J. (1999). A putative exchange factor for Rho1 GTPase is required for initiation of cytokinesis in Drosophila. *Genes Dev.* **13**, 2301-2314.
Przewloka, M. R., Zhang, W., Costa, P., Archambault, V., D'Avino, P. P., Lilley, K. S., Laue, E. D., McAinsh, A. D. and Glover, D. M. (2007). Molecular analysis of core kinetochore composition and assembly in Drosophila melanogaster. *PLoS ONE* **2**, e478.
Raich, W. B., Moran, A. N., Rothman, J. H. and Hardin, J. (1998). Cytokinesis and midzone microtubule organization in Caenorhabditis elegans require the kinesin-like protein ZEN-4. *Mol. Biol. Cell* **9**, 2037-2049.
Saint, R. and Somers, W. G. (2003). Animal cell division: a fellowship of the double ring? *J. Cell Sci.* **116**, 4277-4281.
Somers, W. G. and Saint, R. (2003). A RhoGEF and Rho family GTPase-activating protein complex links the contractile ring to cortical microtubules at the onset of cytokinesis. *Dev. Cell* **4**, 29-39.
Somma, M. P., Fasulo, B., Cenci, G., Cundari, E. and Gatti, M. (2002). Molecular dissection of cytokinesis by RNA interference in *Drosophila* cultured cells. *Mol. Biol. Cell* **13**, 2448-2460.
Straight, A. F., Field, C. M. and Mitchison, T. J. (2004). Anillin binds nonmuscle myosin II and regulates the contractile ring. *Mol. Biol. Cell* **16**, 193-201.
Tatsumoto, T., Xie, X., Blumenthal, R., Okamoto, I. and Miki, T. (1999). Human ECT2 is an exchange factor for Rho GTPases, phosphorylated in G2/M phases, and involved in cytokinesis. *J. Cell Biol.* **147**, 921-928.
Yuce, O., Piekny, A. and Glotzer, M. (2005). An ECT2-centralspindlin complex regulates the localization and function of RhoA. *J. Cell Biol.* **170**, 571-582.
Zavortink, M., Contreras, N., Addy, T., Bejsovec, A. and Saint, R. (2005). Tum/RacGAP50C provides a critical link between anaphase microtubules and the assembly of the contractile ring in Drosophila melanogaster. *J. Cell Sci.* **118**, 5381-5392.
Zhao, W. M. and Fang, G. (2005). MgcRacGAP controls the assembly of the contractile ring and the initiation of cytokinesis. *Proc. Natl. Acad. Sci. USA* **102**, 13158-13163.